HHS Public Access

Author manuscript

Biochem Biophys Res Commun. Author manuscript; available in PMC 2021 January 08.

Published in final edited form as:

Biochem Biophys Res Commun. 2020 January 08; 521(2): 414–419. doi:10.1016/j.bbrc.2019.10.138.

Lysosome-associated membrane protein-2 deficiency increases the risk of reactive oxygen species-induced ferroptosis in retinal pigment epithelial cells

Jong-Jer Lee[a,b,*], **Kenji Ishihara**[a], **Shoji Notomi**[a,c], **Nikolaos E. Efstathiou**[a], **Takashi Ueta**[a], **Daniel Maidana**[a], **Xiaohong Chen**[a], **Yasuhiro Iesato**[a], **Alberto Caligiana**[a], **Demetrios G. Vavvas**[a,**]

[a]Angiogenesis Laboratory, Retina Service, Department of Ophthalmology, Massachusetts Eye and Ear Infirmary, Harvard Medical School, Boston, MA, USA

[b]Department of Ophthalmology, Kaohsiung Chang Gung Memorial Hospital, Kaohsiung, Taiwan

[c]Department of Ophthalmology, Kyushu University, Fukuoka, Japan

Abstract

Lysosome-associated membrane protein-2 (LAMP2), is a highly glycosylated lysosomal membrane protein involved in chaperone mediated autophagy. Mutations of LAMP2 cause the classic triad of myopathy, cardiomyopathy and encephalopathy of Danon disease (DD). Additionally, retinopathy has also been observed in young DD patients, leading to vision loss. Emerging evidence show LAMP2-deficiency to be involved in oxidative stress (ROS) but the mechanism remains obscure. In the present study, we found that *tert*-butyl hydroperoxide or antimycin A induced more cell death in LAMP2 knockdown (LAMP2-KD) than in control ARPE-19 cells. Mechanistically, LAMP2-KD reduced the concentration of cytosolic cysteine, resulting in low glutathione (GSH), inferior antioxidant capability and mitochondrial lipid peroxidation. ROS induced RPE cell death through ferroptosis. Inhibition of glutathione peroxidase 4 (GPx4) increased lethality in LAMP2-KD cells compared to controls. Cysteine and glutamine supplementation restored GSH and prevented ROS-induced cell death of LAMP2-KD RPE cells.

Keywords

AMD; Retinal pigment epithelium; ROS; Ferroptosis; Degeneration; Macula

[*]Corresponding author. Angiogenesis Laboratory, Retina Service, Department of Ophthalmology, Massachusetts Eye and Ear Infirmary, Harvard Medical School, Boston, MA, USA. [**]Corresponding author. tojjlee@cgmh.org.tw (J.-J. Lee), Demetrios_vavvas@meei.harvard.edu (D.G. Vavvas).

Appendix A. Supplementary data

Supplementary data to this article can be found online at https://doi.org/10.1016/j.bbrc.2019.10.138.

Transparency document

Transparency document related to this article can be found online at https://doi.org/10.1016/j.bbrc.2019.10.138

1. Introduction

Lysosome-associated membrane protein-2 (LAMP2), a highly glycosylated protein, is constitutively expressed on lysosomal membrane [1]. Alternative splicing of the LAMP2 gene produces subtypes of the protein: LAMP2A, LAMP2B, and LAMP2C [2]. LAMP2A plays a unique role in chaperone-mediated autophagy [3], LAMP2B participates in macroautophagy [4,5], and LAMP2C is involved in the degradation of RNA or DNA [6,7]. Clinically, LAMP2 mutations cause Danon disease (DD), a monogenic X-linked disorder characterized by the classic triad of cardiomyopathy, myopathy and intellectual disability [8–10]. The inefficient lysosome biogenesis/maturation and impaired autophagosome-lysosome fusion underlies the cardiac and skeletal muscular pathogenesis of DD [4,5,10–12]. In addition to the classic triad, patients with DD may have vision decline from a young age and case reports show disturbances of the retinal pigment epithelium (RPE) [11,13]. Mutation of p.Gly384Arg in LAMP2 induces cone-rod dystrophy [14]. The tight junctions between RPE cells appear to be disabled in DD [15]. LAMP2 deficiency has been shown to also play a role in RPE basolaminar deposits and AMD [25]. Additionally, LAMP2 has also been found to regulate reactive oxygen species (ROS). LAMP2 appears to be required for ROS clearance in zinc treated A549 lung epithelium cells [16] and LAMP2-deficient human brain vascular smooth muscle cells showed mitochondrial fragmentation and overproduction of ROS [17]. However, the exact mechanism of LAMP2 control of ROS has not been investigated in these studies.

Autophagy plays an important role in counteracting ROS in different cell types, including RPE [18,19]. It has been shown that autophagy maintained the GSH: GSSG ratio in ROS-treated RPE cells [20], however the exact role of lysosomal protein LAMP2 under ROS is not fully understood. In the present study, we investigated the effect of oxidative stress on cell survival of RPE cells with and without LAMP2 deficiency and explored the involved cell death mechanism.

2. Materials and methods

2.1. Chemicals and antibodies

Chemicals: *tert*-Butyl hydroperoxide was from Acros Organic (Geel, Belgium). Bovine serum albumin (BSA) was from bioWORLD (Dublin, OH), Tris-buffer saline (TBS) was from Boston Bioproducts, (Ashland, MA). Bafilomycin A1, Deferoxamine, MG-132, ML-162, and (1S,3R)-RSL3 were from Cayman Chemical (Ann Arbor, MI). Sterile DMSO, Protease/Phosphatase Inhibitor Cocktail (#5872) were from Cell Signaling (Danvers, MA). ECL HRP substrate reagents were from GeneTex (Irvine, CA). Retinal Epithelial Cell basal medium (RtEBM) and RtEGM SingleQuots Supplements were from Lonza (Allendale, NJ). 2,2′-bipyridyl, antimycin A, brilliant blue R, glacial acetic acid, L-cysteine, glycine, L-glutamine, and 2-mercaptoethanol were from MilliporeSigma (Burlington, MA). Carbobenzoxy-valyl-alanyl-aspartyl-[O-methyl]-fluoromethylketone (z-VAD-FMK) was from R&D Systems (Minneapolis, MN). Tween-20 were from Santa Cruz (Dallas, TX). Bortezomib and Necrostatin-1 were from Sellek Chemicals (Houston, TX). 4′, 6-diamidino-2′-phenylindole, dihydrochloride (DAPI), Dulbecco's phosphate-buffered saline (DPBS) for cell culture, Dulbecco's Modified Eagle Medium: Nutrient Mixture F-12

(DMEM/F12), fetal bovine serum (FBS, heat-inactivated), Penicillin-Streptomycin, NuPAGE LDS Sample Buffer, Pierce Coomassie (Bradford) protein assay reagent were from Thermo Fisher (Waltham, MA).

Antibodies and probes: ATP6V0D1 (ab202899) and GPx4 (ab125066) were from Abcam (Cambridge, MA). LAMP1 (555798) was from BD (San Jose, CA). ATF4 (#11815), ATG5 (#12994), COX IV (#4850), HSP60 (#12165), xCT (#12691), and HRP-linked secondary antibodies (#7074 and #7076) were from Cell Signaling. Cell Counting Kit-8 (CCK-8) and MitoPeDPP were from Dojindo (Kumamoto, Japan). Tomm20 (MABT166) was from MilliporeSigma. ATP6V1C1 (16054), ATP6V1H (26683), CTNS (13085), GCLC (12601) and GCLM (12601) were from Proteintech (Rosemont, IL). ATP6V1E1 (sc-48375), Ferritin heavy chain (sc-376594), LAMP2 (sc-18822), Rab 7 (sc-376362) were from Santa Cruz. MitoTracker Deep Red FM (M22426) were from Thermo Fisher.

2.2. Cell culture and siRNA transfection

ARPE-19 cells were obtained from ATCC (Manassas, VA). Primary human retinal pigment epithelial cells (hfRPE) were obtained from Lonza. ARPE-19 cells were seeded at high density in 6-well (1.2×10^6 cells), 24-well (3×10^5 cells), or 96-well (5×10^4 cells) transparent plates (Greiner Bio On, Frickenhausen, Germany) to full confluency before experiments. A 96 black-well plate (Cellvis, Mountain View, CA) or eight-well (8×10^4 cells in each well) glass bottom chamber slide (Thermo Fisher) was used when imaging or detection of fluorescent probe was required. The number of seeded cells of hfRPE was double that of ARPE-19 cells. ARPE-19 cells were maintained in DMEM/F-12 with HEPES plus 10% FBS and penicillin-streptomycin (100 U/ml). HfRPE cells were maintained in RtEBM basal medium with RtEGM SingleQuots supplements. Both cell lines were incubated at 37 °C with 5% CO2. All experiments were done with cells that underwent fewer than five passages after thawing from liquid nitrogen. Both cell lines were transfected with three unique 27mer siRNA duplexes specific for human LAMP1 (IDT, Coralville, Iowa), LAMP2 (OriGene, Rockville, MD), or scramble siRNA (OriGene) as the control, using Lipofectamine RNAiMAX Transfection Reagent (Thermo Fisher) according to the manufacturer's protocol. Experiments were carried out 5 days after the transfection procedure. The effectiveness of the LAMP1 and LAMP2 knockdown was examined regularly using western blots.

2.3. ROS induction

Cells were seeded and allowed to grow to confluence before ROS induction. Exogenous ROS were induced chemically with *tert*-Butyl hydroperoxide (tBHP) or antimycin A1 diluted in culture medium, with concentration and duration dependent on the purpose of individual experiments.

2.4. Cell viability assay

Cells were seeded in sterile transparent 96-well plates and cultured until fully confluent for cytotoxic experiments. The culture media was replaced with fresh Phenol red free media 10% (v/v) of CCK-8 reagent and incubated for 2 h at 37 °C in an incubator immediately

after individual experiment. The absorption of the medium was then measured at 450 nm with a SpectraMax 190 microplate spectrophotometer (Molecular Device, San Jose, CA).

2.5. Western blot analysis

Cells were lysed in mammalian protein extraction buffer (M-PER, Thermo Fisher) with protease/phosphatase inhibitor cocktail. The protein concentration was measured using a Pierce Coomassie (Bradford) protein assay. Protein samples was prepared in 4 × NuPAGE LDS sample buffer with 1.25% (v/v) 2-mercaptoethanol and denatured at 90 °C for 5 min. Equal amounts of protein samples were separated on a 4–12% SDS-PAGE Bis-Tris gel (Thermo Fisher) and transferred to PVDF membranes (MilliporeSigma) on a semidry blotting system (GenScript, Piscataway, NJ). Equal protein loading was immediately evaluated with Coomassie blue staining (staining solution: 0.1% Brilliant Blue, 50% methanol and 10% glacial acetic acid) after transfer. The PVDF membrane was then blocked with 2% (w/v) BSA in TBS with Tween-20 (TBST). Next, the membranes were incubated with primary antibodies diluted with TBST and 1% (w/v) BSA overnight at 4 °C and subsequently incubated with HRP-linked secondary antibodies for 1 h at RT. The results were visualized with HRP substrate reagent and detected with an ECL/ChemiDoc imaging system (Bio-Rad, Hercules, CA).

2.6. Cytosolic cysteine concentration

Cytosolic protein was collected from confluent ARPE19 cells in 24-well plates with a subcellular protein fractionation kit (78840, Thermo Fisher). The abundance of cysteine in the cytosolic fraction was determined with a cysteine assay kit using the protocol recommended by manufacturer (K558, Biovision, Milpitas, CA). Fluorescence was detected with a SpectraMax Gemini XS microplate fluorometer. The protein concentrations of each sample were determined by Coomassie protein assay.

2.7. Glutathione assay

To study the effect of amino acid supplementation on intracellular GSH concentration, the culture media of ARPE-19 cells was replaced with serum free DMEM/F12 with or without cysteine (5 mM), glutamine (5 mM), or glycine (2 mM) for 24 h, beginning 4 days following siRNA transfection. Intracellular total glutathione (GSH) level was detected with a glutathione cell-based detection kit (No. 600360, Cayman, Ann Arbor, MI) according to the manufacturer's instructions. Briefly, cells in 24-well plates were lysed, and the soluble proteins were collected to incubate for 2h at RT with monochlorobimane, which reacts with GSH to generate a 480 nm fluorescence when excited with 380 nm light. The protein concentration of each sample was determined using a Coomassie protein assay.

2.8. Lipid peroxidation assays

Lipid peroxidation of whole cell lysate was detected with HNE ELISA. Lysates (M-PER Lysis buffer) of 2×10^5 ARPE-19 cells were collected for each sample. HNE Adduct Competitive ELISA kit was used according to the protocol provided by manufacturer (Cell Biolabs, San Diego, CA). Briefly, the samples were added to the HNE-Conjugate pre-coated plate for short incubation. The primary anti-HNE antibody, HRP-conjugate secondary

antibody, substrate solution and stop solution were incubated with the sample containing well one by one in sequence. The absorption of the reaction mixture was then measured at 450 nm with SpectraMax 190 microplate spectrophotometer. For detection of mitochondrial lipid peroxidation, ARPE-19 cells were seeded in chamber slides. The medium was replaced with serum free DMEM/F12 with or without cysteine (5 mM) supplementation for 24 h starting the day after siRNA transfection. The cells were then stained for 30 min with 100 nM of MitoTracker Deep Red FM and 0.1 μM of MitoPeDPP, a dye that accumulates in mitochondrial inner membranes with lipid peroxidation and emits fluorescence at 470 nm when excited with 420 nm light. The cells were then washed with HBSS and imaged with an Axio Imager M2 microscope (Zeiss).

2.9. Statistical analysis

The data were analyzed statistically to evaluate the differences observed between the control and LAMP2-KD cells using t-tests, one-way analysis of variance (ANOVA), or two-way ANOVA analysis with Tukey's multiple comparisons test using GraphPad 8.0.1 software (San Diego, CA). The significance is reported as NS: not statistically significant, * for $p < 0.05$, ** for $p < 0.01$, and *** for $p < 0.001$ in all figures.

3. Results & discussion

3.1. LAMP2-deficient RPE cells are more susceptible to ROS-induced cell death

To examine the role of LAMP2 in ROS related cell death in ARPE-19 cells we used siRNA to suppress its expression (Fig. S1) and exposed scramble and LAMP2 siRNA treated cells to *tert*-butyl hydroperoxide (tBHP) and antimycin-A to induce non-specific or mitochondrial reactive oxygen species (ROS) respectively. Minimal cell death was observed 24 h after a 3 h exposure with 150 μM tBHP in either control or LAMP2-knockdown (KD) ARPE-19 cells. However, treatment with 300 μM tBHP significantly reduced cell survival rate (45.1%) in LAMP2-knockdown (KD) ARPE-19 cells when compared to that of the control (81.0%). (Fig. 1A, n = 6). Similarly, antimycin A that generates mitochondrial ROS also induced more cell death in LAMP2-KD than in control ARPE-19 cells (Fig. 1B, n = 6).

3.2. ROS induces ferroptosis in LAMP2 deficient RPE cells

Sublethal tBHP (150 μM, 3 h) treatment led to upregulation of genes associated with ferroptosis in ARPE-19 cells as detected by western blot analysis (Fig. 2A, n = 3) suggesting that ferroptosis may be an important cell death mechanism in LAMP2 deficiency and ROS exposure. Indeed, only iron chelator deferoxamine (DFO, 100 μM, 4 h) but not inhibitors for apoptosis (z-VAD-FMK) or necroptosis (Necrostatin-1) prevented LAMP2-KD ARPE-19 cells from ROS-induced death (Fig. 2B, n = 6). Similar to DFO, other inhibitors of ferroptosis, such as fast-reacting iron chelator 2,2′-bipyridyl (BIP) (100 μM, for 4 h) also protected the LAMP2-KD cells from tBHP-induced cell death in both primary fetal retinal pigment epithelium (hfPRE) and ARPE-19 cells (Fig. 2C, n = 6, tBHP: 2 mM, 4 h for hfRPE and 300 μM, 3 h for ARPE-19). The effect of iron-chelation on RPE is in accordance with the findings of a published study of ROS-induced cell death mechanism [21]. The susceptibility of LAMP2-deficent cells to ferroptosis was further supported with the detection of increased sensitivity to ferroptosis inducers. LAMP2-KD, but not control cells,

pretreated with Erastin (10 μM, 12 h) was susceptible to cell death at sub-lethal levels of tBHP (50 μM) (Fig. 2D, n = 6). Ferroptosis has been associated with increased lipid peroxidation. Indeed, lipid peroxidation product *4-hydroxy-2-nonenal* (HNE) was increased in LAMP2 knockdown cells and this upregulation was further increased after tBHP treatment (Fig. 2E, n = 7). As Glutathione peroxidase 4 (GPX4) is an enzyme that protects against membrane lipid peroxidation, GPX4 inhibitors RSL3 (1 μM) and ML-162 (1 μM) were associated with increased cell death in LAMP2-KD compared to control cells (Fig. 2F, n = 6).

3.3. Cysteine and GSH deficiency in LAMP2-knockdown RPE cells

Cysteine is crucial in the regulation of ferroptosis since it is a precursor for glutathione (GSH) synthesis, and GSH is needed for many anti-ferroptosis and antioxidant enzymes. Knockdown of LAMP2 resulted in decreased cytosolic cysteine in ARPE19 cells (Fig. 3A, n = 8). The shortage of cysteine was further associated with likely compensatory mild upregulation of Activating Transcription Factor 4 (ATF4) which regulates key biosynthetic enzymes for cysteine; this upregulation was alleviated after cysteine supplementation (Fig. 3B, n = 3).

As cysteine is a precursor to GSH, LAMP2 deficient cells had a reduction in GSH (Fig. 3C). This GSH reduction in LAMP2 KD cells was prevented with supplementation of L-cysteine (Cys, 5 mM). Addition of L-glutamine (Gln, 5 mM) that can be converted into glutamate intracellularly, further promoted the GSH synthesis (Fig. 3C, n = 6). Furthermore, pretreatment with cysteine and glutamine (5 mM each) for 24 h significantly reduced tBHP-induced cell death in LAMP2-KD cells (Fig. 3D). The effect of Cys and Gln amino acid supplementation was abolished with L-Buthionine-(S, R)-sulfoximine (BSO, 1 mM) which impairs GSH synthesis through inhibition of glutamate-cysteine ligase (Fig. 3D, n = 4).

Autophagy has been shown to be an important cellular mechanism for amino acid utility and could be partially responsible for the changes in the levels of cysteine in LAMP2 knockdown cells. Unexpectedly, in the duration of LAMP2 downregulation of our experiments we did not observe significant change of autophagy flux in either ARPE-19 or hfRPE (Fig. S2). Therefore, cysteine and GSH shortage may happen before the impairment of autophagy flux and could be caused by other mechanisms in LAMP2-KD RPE, at least for the time frame examined of this study.

3.4. Downregulation of V-ATPase in LAMP2-KD RPE

The utility, synthesis, and conversion between amino acids in cell involve crosstalk between sophisticated systems, including autophagosomes and lysosomes [22,23]. Lysosomes may work as a reservoir that regulate hemostasis of intracellular cysteine. V-ATPase, which maintains the proton gradient in the lysosome, is essential for the transport of cystine -a precursor of cysteine-from lysosome into cytosol through cystinosin (CTNS) [23]. In our study we found that in RPE, the subunits of the cytosolic V1 domain of V-ATPase were downregulated (Fig. 4A, n = 3). The downregulation of V-ATPase subunits in LAMP2-KD cells was mitigated with Bortezomib (10 nM, 24 h) and MG-132 (10 μM, 24 h) (Fig. 4B, n = 3), suggesting proteasome activity is partially responsible for this reduction. Thus we

speculate that V-ATPase activity may be suboptimal and impairs the transportation and availability of cysteine in LAMP2-KD RPE. Our finding contrasts with studies in LAMP2-deficient mouse hepatocytes which found that the acidification of the autophagic vacuole and multivesicular endosome were not impaired [24]. Therefore, the downregulation of V-ATPase subunits in LAMP2-deficient RPE could be tissue or cell-type specific.

In summary, our results reveal that LAMP2 deficiency decreases the antioxidant capacity of RPE cells, impairs mitochondrial health (Fig. S3) and increases ROS-induced ferroptotic cell death at least partially through a reduction in cysteine, GSH and V-ATPase. Iron chelation and cysteine supplementation could be useful for retinal protection in patients with DD. Furthermore, since both autophagy dysfunction and LAMP2 reduction are seen with aging [25–27], further enquiry into the role of iron chelation and GPx4 activation in degenerative diseases involving LAMP2 dysfunction is needed.

Supplementary Material

Refer to Web version on PubMed Central for supplementary material.

Acknowledgements

This work was supported by the Yeatts Family Foundation (D.G.V.); Monte J. Wallace (DGV) 2013 Macula Society Research Grant award (D.G.V.); a Physician Scientist Award by the Research to Prevent Blindness Foundation (D.G.V.); Robert Machemer Foundation Vitreoretinal Research Scholarship (SN); NEI R21EY023079–01/A1 (D.G.V.); NEI grant EY014104 (MEEI Core Grant); Loeffler Family fund (D.G.V.); R01EY025362–01 (D.G.V.); ARI Young investigator Award (D.G.V.); Foundation Lions Eye Research Fund (D.G.V.); NIH NEI Core grant P30EY003790 (D.G.V.)

References

[1]. Granger BL, Green SA, Gabel CA, Howe CL, Mellman I, Helenius A, Characterization and cloning of lgp110, a lysosomal membrane glycoprotein from mouse and rat cells, J. Biol. Chem 265 (1990) 12036–12043. [PubMed: 2142158]

[2]. Eskelinen E-L, Cuervo AM, Taylor MRG, Nishino I, Blum JS, Dice JF, V Sandoval I, Lippincott-Schwartz J, August JT, Saftig P, Unifying nomenclature for the isoforms of the lysosomal membrane protein LAMP-2, Traffic 6 (2005) 1058–1061, 10.1111/j.1600-0854.2005.00337.x. [PubMed: 16190986]

[3]. Bandyopadhyay U, Kaushik S, Varticovski L, Cuervo AM, The chaperone-mediated autophagy receptor organizes in dynamic protein complexes at the lysosomal membrane, Mol. Cell. Biol 28 (2008) 5747–5763, 10.1128/MCB.02070-07. [PubMed: 18644871]

[4]. Tanaka Y, Guhde G, Suter A, Eskelinen EL, Hartmann D, Lullmann-Rauch R, Janssen PM, Blanz J, von Figura K, Saftig P, Accumulation of autophagic vacuoles and cardiomyopathy in LAMP-2-deficient mice, Nature 406 (2000) 902–906, 10.1038/35022595. [PubMed: 10972293]

[5]. Rowland TJ, Sweet ME, Mestroni L, Taylor MRG, Danon disease e dysregulation of autophagy in a multisystem disorder with cardiomyopathy, J. Cell Sci 129 (2016) 2135–2143, 10.1242/jcs.184770. [PubMed: 27165304]

[6]. Fujiwara Y, Furuta A, Kikuchi H, Aizawa S, Hatanaka Y, Konya C, Uchida K, Yoshimura A, Tamai Y, Wada K, Kabuta T, Discovery of a novel type of autophagy targeting RNA, Autophagy 9 (2013) 403–409, 10.4161/auto.23002. [PubMed: 23291500]

[7]. Fujiwara Y, Kikuchi H, Aizawa S, Furuta A, Hatanaka Y, Konya C, Uchida K, Wada K, Kabuta T, Direct uptake and degradation of DNA by lysosomes, Autophagy 9 (2013) 1167–1171, 10.4161/auto.24880. [PubMed: 23839276]

[8]. Danon MJ, Oh SJ, DiMauro S, Manaligod JR, Eastwood A, Naidu S, Schliselfeld LH, Lysosomal glycogen storage disease with normal acid maltase, Neurology 31 (1981) 51–57. [PubMed: 6450334]

[9]. Nishino I, Fu J, Tanji K, Yamada T, Shimojo S, Koori T, Mora M, Riggs JE, Oh SJ, Koga Y, Sue CM, Yamamoto A, Murakami N, Shanske S, Byrne E, Bonilla E, Honaka I, DiMauro S, Hirano M, Primary LAMP-2 deficiency causes X-linked vacoular cardiomyopathy and myopathy (Danon disease), Nature 406 (2000) 906–910, 10.1038/35022604. [PubMed: 10972294]

[10]. Endo Y, Furuta A, Nishino I, Danon disease: a phenotypic expression of LAMP-2 deficiency, Acta Neuropathol 129 (2015) 391e398, 10.1007/s00401-015-1385-4.

[11]. He J, Wang Y, Jiang T, Danon disease: a novel mutation in the LAMP-2 gene and ophthalmic abnormality, Herz 39 (2013) 877–879, 10.1007/s00059-013-3900-5. [PubMed: 23955649]

[12]. Nascimbeni AC, Fanin M, Angelini C, Sandri M, Autophagy dysregulation in Danon disease, Cell Death Dis 8 (2017), 10.1038/cddis.2016.475.

[13]. Prall FR, Drack A, Taylor M, Ku L, Olson JL, Gregory D, Mestroni L, Mandava N, Ophthalmic manifestations of Danon disease, Ophthalmology 113 (2006) 1010–1013, 10.1016/j.ophtha.2006.02.030. [PubMed: 16751040]

[14]. Thiadens AAHJ, Slingerland NWR, Florijn RJ, Visser GH, Riemslag FC, Klaver CCW, Cone-rod dystrophy can be a manifestation of Danon disease, Graefe's Arch. Clin. Exp. Ophthalmol 250 (2012) 769–774, 10.1007/s00417-011-1857-8. [PubMed: 22290069]

[15]. Thompson DA, Constable PA, Liasis A, Walters B, Esteban MT, The physiology of the retinal pigment epithelium in Danon disease, Retina 36 (2016) 629–638, 10.1097/IAE.0000000000000736. [PubMed: 26398689]

[16]. Qin X, Zhang J, Wang B, Xu G, Zou Z, LAMP-2 mediates oxidative stress-dependent cell death in Zn2+-treated lung epithelium cells, Biochem. Biophys. Res. Commun 488 (2017) 177–181, 10.1016/j.bbrc.2017.05.030. [PubMed: 28483530]

[17]. Nguyen HT, Noguchi S, Sugie K, Matsuo Y, Nguyen CTH, Koito H, Shiojima I, Nishino I, Tsukaguchi H, Small-vessel vasculopathy due to aberrant autophagy in LAMP-2 deficiency, Sci. Rep 8 (2018), 10.1038/s41598-018-21602-8.

[18]. Dutta D, Xu J, Kim JS, Dunn WA, Leeuwenburgh C, Upregulated autophagy protects cardiomyocytes from oxidative stress-induced toxicity, Autophagy 9 (2013) 328–344, 10.4161/auto.22971. [PubMed: 23298947]

[19]. Sureshbabu A, Ryter SW, Choi ME, Oxidative stress and autophagy: crucial modulators of kidney injury, Redox Biol 4 (2015) 208–214, 10.1016/j.redox.2015.01.001. [PubMed: 25613291]

[20]. Mitter SK, Song C, Qi X, Mao H, Rao H, Akin D, Lewin A, Grant M, Dunn W, Ding J, Rickman CB, Boulton M, Dysregulated autophagy in the RPE is associated with increased susceptibility to oxidative stress and AMD, Autophagy 10 (2014) 1989e2005, 10.4161/auto.36184. [PubMed: 25484094]

[21]. Totsuka K, Ueta T, Uchida T, Roggia MF, Nakagawa S, Vavvas DG, Honjo M, Aihara M, Oxidative stress induces ferroptotic cell death in retinal pigment epithelial cells, Exp. Eye Res 181 (2018) 316–324, 10.1016/j.exer.2018.08.019. [PubMed: 30171859]

[22]. Carroll B, Korolchuk VI, Sarkar S, Amino acids and autophagy: cross-talk and co-operation to control cellular homeostasis, Amino Acids 47 (2015) 2065–2088, 10.1007/s00726-014-1775-2. [PubMed: 24965527]

[23]. Bröer S, Bröer A, Amino acid homeostasis and signalling in mammalian cells and organisms, Biochem. J 474 (2017) 1935e1963, 10.1042/BCJ20160822. [PubMed: 28546457]

[24]. Eskelinen E-L, Role of LAMP-2 in lysosome biogenesis and autophagy, Mol. Biol. Cell 13 (2002) 3355–3368, 10.1091/mbc.E02-02-0114. [PubMed: 12221139]

[25]. Notomi S, Ishihara K, Efstathiou N, et al., Genetic LAMP2 deficiency accelerates the age-associated formation of basal laminar deposits in the retina, Proc. Natl. Acad. Sci. U.S.A (2019). In press.

[26]. Cuervo AM, Dice JF, Age-related decline in chaperone-mediated autophagy, J. Biol. Chem 275 (40) (2000) 31505–31513. [PubMed: 10806201]

[27]. Zhang C, Cuervo AM, Restoration of chaperone-mediated autophagy in aging liver improves cellular maintenance and hepatic function, Nat. Med 14 (9) (2008 9) 959–965, 10.1038/nm.1851. [PubMed: 18690243]

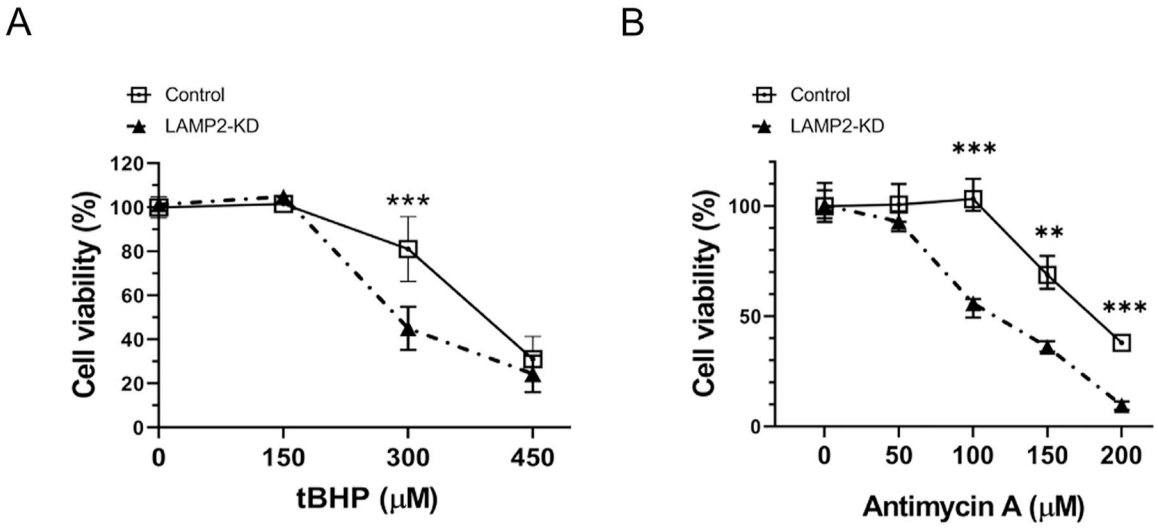

Fig. 1. LAMP2 knockdown (LAMP2-KD) ARPE-19 cells are less resistant to reactive oxygen species (ROS)-induced cell death.

(*A*–*B*) tBHP (3 h) and antimycin A (24 h) induced ARPE-19 cell death as assesed by CCK-8 assay 24 after exposure with inciting agent. Data are expressed as mean ± standard deviation (SD). *p < 0.05, **p < 0.001, ***p < 0.0001, ns: not significant, compared with other groups using ANOVA and Tukey's multiple comparison test.

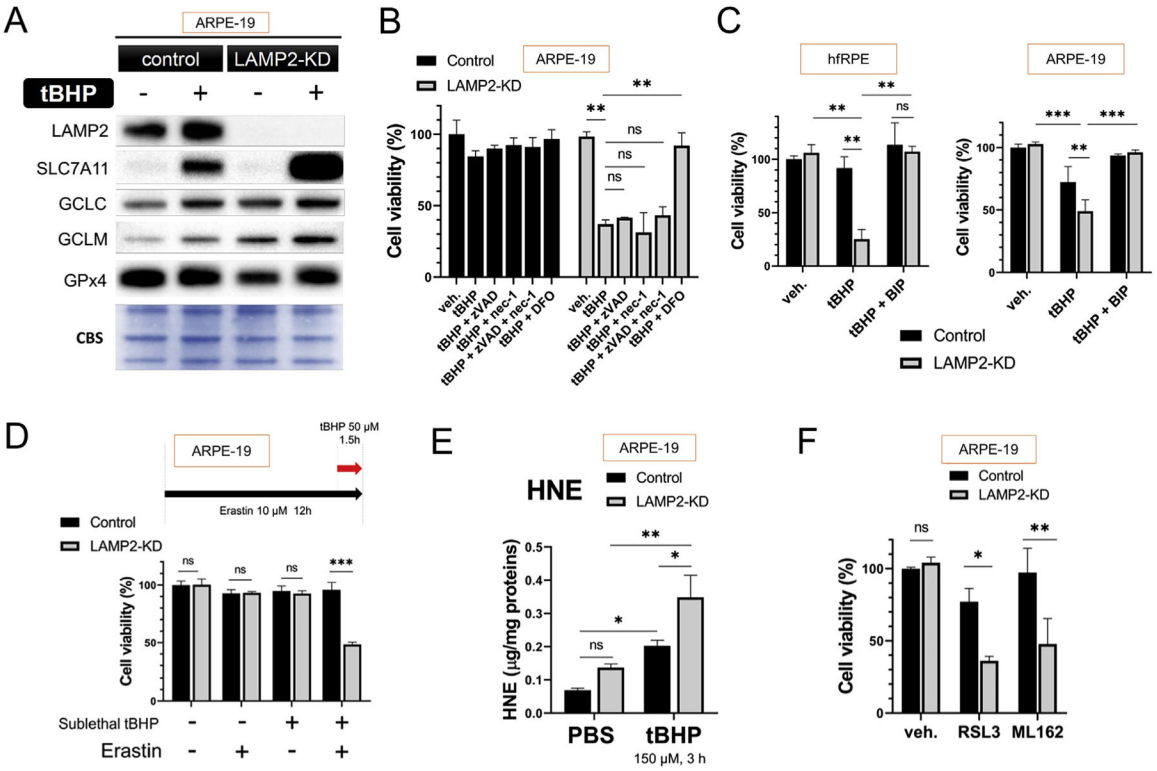

Fig. 2. LAMP2 knockdown RPE cells are susceptible to ROS-induced ferroptosis.

(A) Representative image of western blot (WB) for tBHP-induced anti-ferroptosis proteins in ARPE-19 cells. Cell extracts were collected 24 h after initiation of tBHP (150 μM) exposure for 3h (n = 3), (B) Effects of inhibitors for different cell death modalities on tBHP-induced ARPE-19 cell death; tBHP (300 μM, 3 h), (Nec-1 and zVAD 30 μM each, 4 h pretreatment), (DFO, 100 mM, 4 h pretreatment), viability checked at 24 h (n = 6). (C) Effect of iron chelator 2,2′-bipyridyl (BIP) (100 μM, for 4 h) on tBHP-induced cell death in hfRPE and ARPE-19 cells (n = 6), (D) The effect of Erastin, a cystine/glutamate transporter (xCT) inhibitor, on sublethal tBHP-induced cell death in ARPE-19 cells; (Erastin 10 μM, 12 h ; tBHP 50 μM) (n = 6), (E) HNE level 24 h after 3 h of tBHP (150 μM) in control and LAMP2-KD cells. HNE, 4-hydroxy-2-nonenal. (F) GPx4 inhibitors RSL3 and ML-162 (1 μM for each, 2 h exposure) induced cell death measured 24 h after inhibitor application (n = 6). CBS, Coomassie blue stain. Data are expressed as mean ± standard deviation (SD). *p < 0.05, **p < 0.001, ***p < 0.0001, ns: not significant, compared with other groups using ANOVA and Tukey's multiple comparison test.

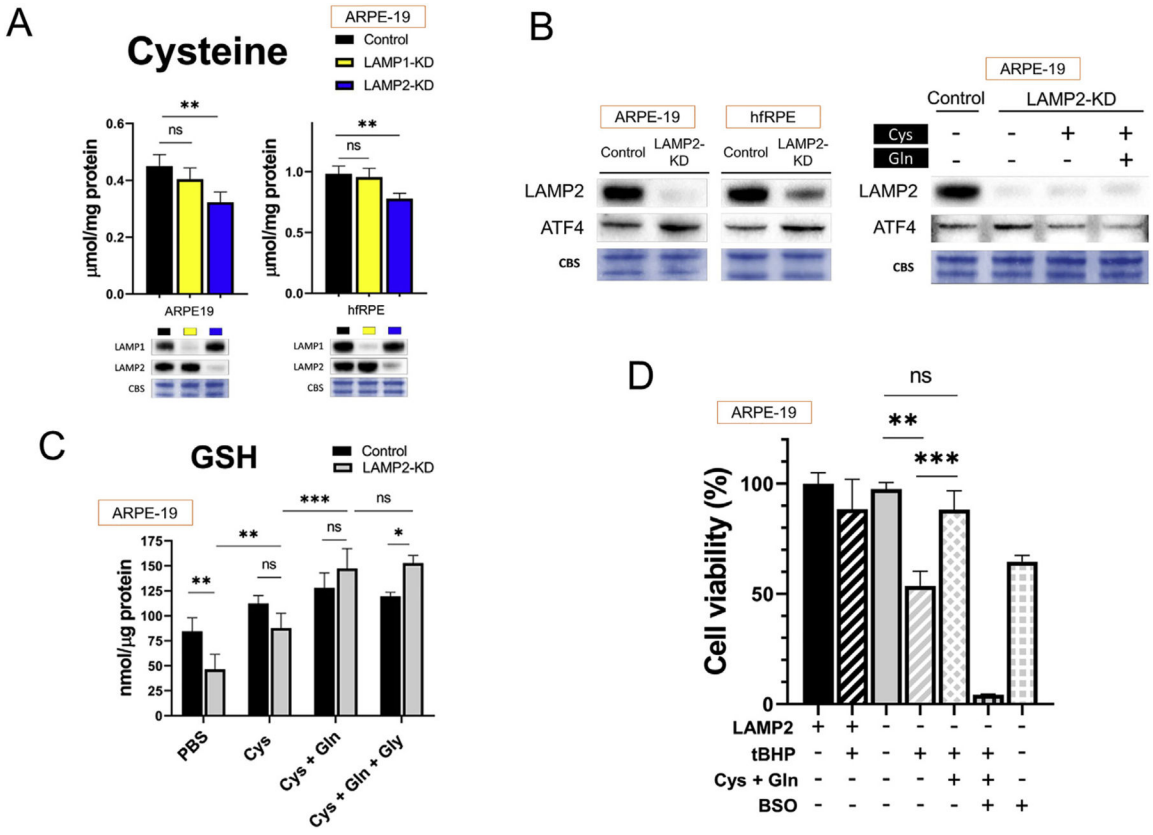

Fig. 3. Cysteine and GSH deficiency in LAMP2-KD ARPE-19 cells.

(A) Cytosolic cysteine level in LAMP1-KD and LAMP2-KD cells 5 days after siRNA exposure (n = 6), (B) Representative image of WB for stress responder ATF4 protein 5 days after siRNA exposure (n = 3), (C) Effect of cysteine (5 mM) glutamine (5 mM) and glycine (2 mM) supplementation for 24 h on intracellular GSH level (n = 6) and (D) tBHP-induced cell death after pretreatment with cysteine and glutamine (5 mM each) for 24 h. The effect of Cys and Gln amino acid supplementation was abolished with l-Buthionine-(S, R)-sulfoximine (BSO, 1 mM, 4 h pretreatment); viability checked at 24 h, tBHP at 300 µM (n = 6). Data are expressed as mean ± standard deviation (SD). *p < 0.05, **p < 0.001, ***p < 0.0001, ns: not significant, compared with other groups using ANOVA and Tukey's multiple comparison test.

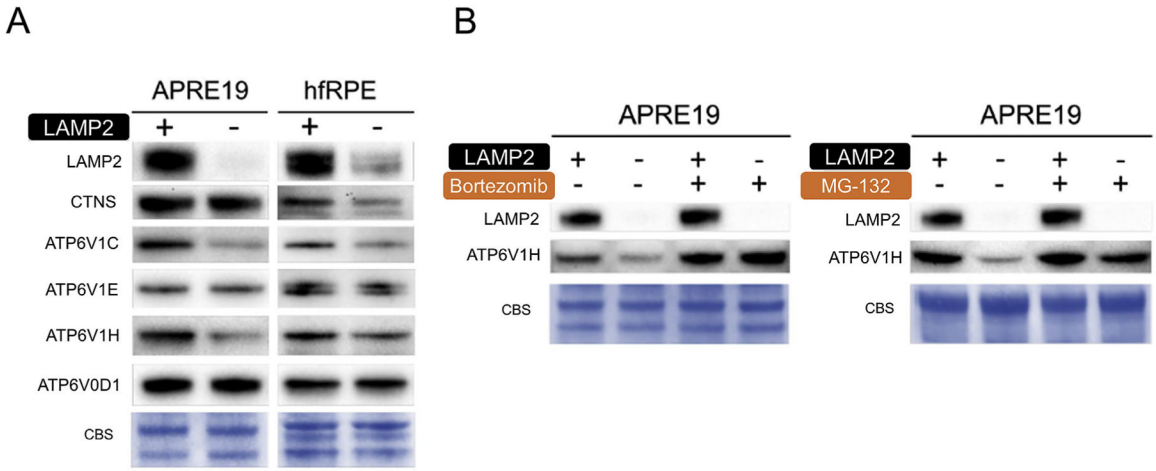

Fig. 4. Down regulation of V-ATPase in LAMP2-KD RPE.

(A) Representative WB image for protein levels of CTNS and components of V-ATPase in RPE cells 5 days after siRNA exposure (n = 3), (B) Representative WB image for the effect of proteasome inhibition on V-ATPase subunit H protein expression 5 days after siRNA exposure (Inhibitors applied at day 4 for 24 h) (n = 3). V-ATPase, vacuolar-type H + ATPase; CTNS, cystinosin.